Building Three-Dimensional Differentiable Manifolds Numerically II: Limitations

Lee Lindblom[a,b,*], Oliver Rinne[c]

[a] *Center for Astrophysics and Space Sciences, University of California at San Diego, 9500 Gilman Drive, La Jolla, CA 92093, USA*
[b] *Center for Computational Mathematics, University of California at San Diego, 9500 Gilman Drive, La Jolla, CA 92093, USA*
[c] *Faculty 4, HTW Berlin – University of Applied Sciences, Treskowallee 8, 10318 Berlin, Germany*

1. Summary

Methods were developed in Ref. [1] for constructing reference metrics (and from them differentiable structures) on three-dimensional manifolds with topologies specified by suitable triangulations. This note generalizes those methods by expanding the class of suitable triangulations, significantly increasing the number of manifolds to which these methods apply. These new results show that this expanded class of triangulations is still a small subset of all possible triangulations. This demonstrates that fundamental changes to these methods are needed to further expand the collection of manifolds on which differentiable structures can be constructed numerically.

2. Fixing the Dihedral Angles

The method for constructing reference metrics in Ref. [1] begins with the construction of a flat metric in the neighborhood of each vertex of a multicube structure, which can be obtained from a triangulation of that manifold. These flat metrics are then combined using partition of unity functions to produce a global C^0 metric, and then smoothed to C^1 by a sequence of additional steps described in Ref. [1]. These flat metrics are constructed by fixing the dihedral angles of each cube edge. The simple method used in Ref. [1] fixes those dihedral angles to be $2\pi/K$, where K is the number of cube edges that intersect along a particular edge. This choice ensures the sum of the dihedral angles around each edge is 2π, the condition needed to avoid a conical singularity there. This uniform dihedral angle condition severely limits the class of multicube structures on which it can be applied. This simple condition is replaced here with more complicated but less restrictive conditions.

The basic adjustable parameters that determine these flat metrics are the dihedral angles, $\psi_{A\{\alpha\beta\}}$, where the index $A \in \langle 1, ..., N_{\rm cubes}\rangle$ labels the cubes in the multicube structure and $\{\alpha\beta\} \in \langle\{-x-y\},\{-x+y\},\{-x-z\},\{-x+z\},\{+x-y\},\{+x+y\},\{+x-z\},\{+x+z\},\{-y-z\},\{-y+z\},\{+y-z\},\{+y+z\}\rangle$ labels the edge formed by the intersection of the $\{\alpha\}$ and $\{\beta\} \in \langle\{-x\},\{+x\},\{-y\},\{+y\},\{-z\},\{+z\}\rangle$

*Corresponding author
Email addresses: llindblom@ucsd.edu (Lee Lindblom), oliver.rinne@htw-berlin.de (Oliver Rinne)

faces of that cube. Each cube has 12 edges so there are a total of $12N_{\rm cubes}$ dihedral angle parameters needed to determine the vertex centered flat metrics.

The sum of the dihedral angles, $\psi_{A\{\alpha\beta\}}$, from the cubes that intersect along an edge must equal 2π to avoid a conical singularity along that edge. This constraint can be written explicitly:

$$0 = \mathscr{C}_{A\{\alpha\beta\}} \equiv 2\pi - \sum_{A'\{\alpha'\beta'\}} \psi_{A'\{\alpha'\beta'\}} \,, \tag{1}$$

where the sum is over all the edges that intersect along edge $A\{\alpha\beta\}$. Many of these $12N_{\rm cubes}$ constraints are redundant, but for simplicity all are enforced in the numerical analysis here.

Another set of important angles are the vertex angles between the edges of the cube, see Fig. 1. The notation $\theta_{A\{\gamma\}\{\alpha\beta\}}$ is used for these angles, where the A index labels the cube, $\{\gamma\}$ one of the cube faces, and $\{\alpha\beta\}$ the edge that intersects $\{\gamma\}$ at the $\{\alpha\beta\gamma\}$ vertex. These $\theta_{A\{\gamma\}\{\alpha\beta\}}$ are the angles between vectors tangent to the $\{\alpha\gamma\}$ and the $\{\beta\gamma\}$ edges. There are three vertex angles $\theta_{A\{\gamma\}\{\alpha\beta\}}$ associated with each vertex, so 24 for each cube and $24N_{\rm cubes}$ total for the multicube structure. The law of cosines from spherical trigonometry gives the relationship between a vertex angle $\theta_{A\{\gamma\}\{\alpha\beta\}}$ and the dihedral angles $\psi_{A\{\alpha\beta\}}$ associated with the cube edges that intersect at that vertex:

$$\cos\theta_{\{\gamma\}\{\alpha\beta\}} = \frac{\cos\psi_{\{\alpha\beta\}} - \cos\psi_{\{\alpha\gamma\}}\cos\psi_{\{\beta\gamma\}}}{\sin\psi_{\{\alpha\gamma\}}\sin\psi_{\{\beta\gamma\}}} \,. \tag{2}$$

The $\theta_{A\{\gamma\}\{\alpha\beta\}}$ can therefore be considered functions of the $\psi_{A\{\alpha\beta\}}$.

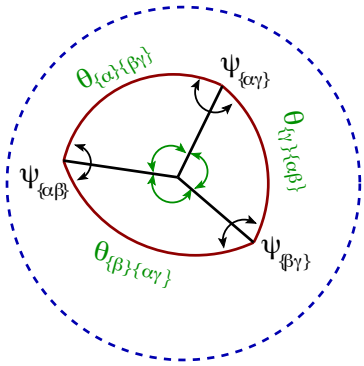

Figure 1: Figure shows the intersection between the corner of a cubic region and a small sphere centered on one of the vertices of that cube. This sphere is depicted as the dashed (blue) curve; the intersection of this cubic region with the sphere is a spherical triangle shown as solid (red) curves; the solid (black) straight lines are the edges of the cube. The dihedral angles $\psi_{\{\alpha\beta\}}$ between the cube faces are also the angles of this spherical triangle. The vertex angles, $\theta_{\{\alpha\}\{\beta\gamma\}}$, are the angles between the edges of the cube, and are also the arc lengths of the sides of this spherical triangle.

Consider two cube faces, $A\{\alpha\}$ and $A'\{\alpha'\}$ that are identified in the multicube structure. The intrinsic metrics associated with these cube faces can only be continuous across the interface between cubes if the vertex angles $\theta_{A\{\alpha\}\{\beta\gamma\}}$ are the same as the corresponding angles $\theta_{A'\{\alpha'\}\{\beta'\gamma'\}}$ on the identified face. These additional constraints on the dihedral angles $\psi_{A\{\alpha\beta\}}$ can be written:

$$0 = \mathscr{C}_{A\{\alpha\}\{\beta\gamma\}} \equiv \cos\theta_{A\{\alpha\}\{\beta\gamma\}} - \cos\theta_{A'\{\alpha'\}\{\beta'\gamma'\}} \,. \tag{3}$$

Any interface with $\mathscr{C}_{A\{\alpha\}\{\beta\gamma\}} \neq 0$ has a metric discontinuity and consequently a curvature singularity at that interface. Half of these vertex angle constrains are redundant, but for simplicity all are enforced in the numerical analysis here.

In any multicube structure the N_{edges} independent constraints in Eq. (1) (where N_{edges} are the number of independent edges in the multicube structure) and the $12N_{\text{cubes}}$ independent constraints in Eq. (3) must be satisfied by the $12N_{\text{cubes}}$ dihedral angle parameters. Since there are more constraints than freely specifiable parameters, we expect that many (most) multicube structures will not admit solutions to all the constraints. When solutions do exist we expect they are likely to be unique in most cases. In Ref. [1] a relatively small collection of multicube structures were found that admit uniform dihedral angle solutions to these constraints. Solutions that do not satisfy the uniform dihedral angle condition are found here for a wider class of manifolds.

The vertex angle constraints, Eq. (3), are very nonlinear, and general analytic solutions are not known. More general solutions can be found numerically, however, by finding the minima of the combined constraint norm, $\|\mathscr{C}\|$, defined by

$$\|\mathscr{C}\|^2 = \sum_{A\{\alpha\beta\}} \mathscr{C}^2_{A\{\alpha\beta\}} + \sum_{A\{\gamma\}\{\alpha\beta\}} \mathscr{C}^2_{A\{\gamma\}\{\alpha\beta\}} \,, \tag{4}$$

where the sums are over the $12N_{\text{cubes}}$ edge and the $24N_{\text{cubes}}$ vertex angle constraints defined in Eqs. (1) and (3). This norm is a function of the dihedral angles, $\|\mathscr{C}\|^2 = \|\mathscr{C}(\psi_{A\{\alpha\beta\}})\|^2$ that is bounded below by zero, so a minimum always exists. If $\min \|\mathscr{C}\|^2 = 0$ then all the constraints are satisfied. If $\min \|\mathscr{C}\|^2 \neq 0$ then the constraints are not satisfied and it is not possible to build a non-singular C^0 metric on that multicube structure in this way.

The numerical search for a minimum of $\|\mathscr{C}\|^2$ was started by setting initial guesses for $\psi_{A\{\alpha\beta\}}$ to their uniform dihedral angle values: $\psi_{A\{\alpha\beta\}} = 2\pi/K_{A\{\alpha\beta\}}$, where $K_{A\{\alpha\beta\}}$ is the number of cube edges that intersect edge $A\{\alpha\beta\}$. The numerical search for a minimum was carried out using the Broyden–Fletcher–Goldfarb–Shanno (BFGS) algorithm [2, p. 136] in the Python library `scipy.optimize`. Any numerical minimum with $\|\mathscr{C}\| \leq 10^{-12}$ was considered to be a good numerical solution to all the constraints, while any minimum with $\|\mathscr{C}\| > 10^{-12}$ was rejected. Our interest is finding solutions to these constraints that can be used to construct reference metrics on these manifolds. Our numerical searches for solutions were concentrated near the uniform dihedral angle state, because only relatively undistorted multicube structures are useful to us as computational domains for solving partial differential equations numerically.

Constraint-satisfying dihedral angles $\psi_{A\{\alpha\beta\}}$ were searched for numerically on the 744 multicube structures constructed from the triangulations having eight or fewer tetrahedra included in the Regina [3] catalog of compact orientable three-dimensional manifolds. Table 1 lists the 23 manifolds from this search that satisfy all the constraints as well as the uniform dihedral angle condition. Table 2 lists 80 additional manifolds that admit non-uniform dihedral angle solutions with $\|\mathscr{C}\| \leq 10^{-12}$. The manifold names used in these tables are those from the Regina [3] catalog. These tables also list the number of multicube regions, N_{cubes}, and the maximum number of edges, $K_{\max} = \max K_{A\{\alpha\beta\}}$, that overlap in each multicube structure. Table 2 also includes two parameters, $\min \mathcal{A}_{A\{\alpha\beta\gamma\}}$ and $\min \det g^{-1}_{A\{\alpha\beta\gamma\}}$, that measure how distorted the constraint-satisfying dihedral angles make each multicube region. The quantity $\mathcal{A}_{A\{\alpha\beta\gamma\}}$ is the solid angle subtended by the cube at the $A\{\alpha\beta\gamma\}$ vertex (i.e. the area of the spherical triangle in Fig. 1). This solid angle would equal $\frac{\pi}{2}$ in an un-distorted cube, so $\frac{2}{\pi} \min \mathcal{A}_{A\{\alpha\beta\gamma\}}$ is a good measure of the maximum distortion in a multicube structure. The quantity $\det g^{-1}_{A\{\alpha\beta\gamma\}}$ represents the determinant of the inverse C^0 metric constructed in Ref. [1] from the dihedral angles, evaluated at the vertex $A\{\alpha\beta\gamma\}$. This determinant would equal one in an un-distorted cube, so $\min \det g^{-1}_{A\{\alpha\beta\gamma\}}$ is another good measure of the maximum distortion in a multicube structure. Multicube structures with $\frac{2}{\pi} \min \mathcal{A}_{A\{\alpha\beta\gamma\}} < 10^{-6}$ or $\min \det g^{-1}_{A\{\alpha\beta\gamma\}} < 10^{-6}$ were excluded from the list in Table 2.

These results show that only a small fraction, $(23 + 80)/744 \approx 0.138$, of the multicube structures constructed from eight or fewer triangulations in the Regina [3] catalog allow dihedral angles that satisfy all the constraints. These include only three manifolds constructed from eight tetrahedra, and an even smaller fraction is expected for the manifolds based on triangulations with more tetrahedra. These results reveal that the methods developed in Ref. [1], including the generalizations presented here, are unfortunately quite limited in their ability to construct reference metrics on all the manifolds based on the triangulations in the Regina [3] catalog.

Table 1: Multicube Structures Admitting Uniform Dihedral Angles. The manifold names used here are those from the Regina catalog. Those names are explained in detail in the documentation to the Regina cagalog [3] and also in Ref. [1].

Manifold	N_{cubes}	K_{max}	Manifold	N_{cubes}	K_{max}
L(5,2)	4	4	SFS[RP2/n2:(2,1)(2,-1)]	24	6
L(8,3)	8	4	SFS[S2:(2,1)(2,1)(2,-1)]	8	4
L(10,3)	12	6	SFS[S2:(2,1)(2,1)(3,-2)]	12	6
L(12,5)	12	6	SFS[S2:(2,1)(2,1)(4,-3)]	16	8
L(16,7)	16	8	SFS[S2:(2,1)(2,1)(5,-4)]	20	10
L(20,9)	20	10	SFS[S2:(2,1)(2,1)(6,-5)]	24	12
L(24,11)	24	12	SFS[S2:(2,1)(2,1)(7,-6)]	28	14
L(28,13)	28	14	SFS[S2:(2,1)(2,1)(8,-7)]	32	16
L(32,15)	32	16	SFS[S2:(2,1)(3,1)(5,-4)]	20	5
T×S1	24	6	SFS[S2:(2,1)(3,2)(3,-1)]	20	5
KB/n2×~S1	24	6	SFS[S2:(2,1)(4,1)(4,-3)]	24	6
			SFS[S2:(3,1)(3,1)(3,-2)]	24	6

3. Discussion

Given a set of constraint-satisfying dihedral angles $\psi_{A\{\alpha\beta\}}$, a global C^0 reference metric can be constructed in a straightforward way using the methods developed in Ref. [1]. These C^0 reference metrics determine a basic C^1 differentiable structure on those manifolds. Smoother differentiable structures are needed, however, to allow global solutions to second-order equations like Einstein's gravitational field equation. Methods for transforming the C^0 reference metrics to C^1 (or smoother via Ricci flow) are also given in Ref. [1]. Those methods were used here successfully to construct C^1 reference metrics for the 23 manifolds listed in Table 1 and the 17 manifolds displayed in boldface in Table 2. The constraint-satisfying dihedral angles make the remaining 63 non-boldface manifolds in Table 2 so distorted that non-singular C^1 metrics could not be constructed in this way. Considerable effort was expended in various attempts to find improved methods that could produce non-singular C^1 metrics in those cases, but all those efforts failed. Only $23 + 17$ of the 744 triangulations from the Regina [3] catalog produced C^1 reference metrics that could be used to solve Einstein's equation on those manifolds. These results demonstrate that the methods developed in Ref. [1], and generalized here, are very limited. Expanding the class of manifolds on which useful C^1 reference metrics can be constructed will probably require new methods for transforming the triangulations on those manifolds into ones that cover those manifolds more "uniformly" and so admit less distorted multicube structures.

Acknowledgments

Research was supported by NSF grant 2012857 to the University of California at San Diego.

Table 2: Multicube Structures Admitting Non-uniform Dihedral Angles With $\|\mathscr{C}\| \leq 10^{-12}$. The quantities $\frac{2}{\pi}\min\mathcal{A}$ and $\min\det g^{-1}$ (defined in the text) measure distortion of the multicube structure, with $\frac{2}{\pi}\min\mathcal{A} = \min\det g^{-1} = 1$ in an undistorted structure. Bold face entries also admit non-singular C^1 metrics.

Manifold	N_{cubes}	$K_{\max}$	$\frac{2}{\pi}\min\mathcal{A}$	$\min\det g^{-1}$	Manifold	N_{cubes}	$K_{\max}$	$\frac{2}{\pi}\min\mathcal{A}$	$\min\det g^{-1}$
L(7,2)	**8**	**5**	**0.652**	**0.380**	L(50,19)	24	7	0.117	0.026
L(11,3)	**12**	**6**	**0.424**	**0.202**	L(55,21)	24	6	0.121	0.027
L(13,3)	16	8	0.169	0.036	**SFS[S2:(2,1)(2,1)(2,1)]**	**16**	**5**	**0.332**	**0.495**
L(13,5)	**12**	**5**	**0.598**	**0.500**	SFS[S2:(2,1)(2,1)(2,3)]	20	7	0.228	0.125
L(14,3)	16	8	0.122	0.016	SFS[S2:(2,1)(2,1)(2,5)]	24	9	0.198	0.125
L(15,4)	16	6	0.360	0.112	SFS[S2:(2,1)(2,1)(2,7)]	28	11	0.122	0.073
L(17,4)	20	8	0.188	0.021	**SFS[S2:(2,1)(2,1)(3,-1)]**	**16**	**5**	**0.332**	**0.495**
L(17,5)	16	7	0.358	0.198	**SFS[S2:(2,1)(2,1)(3,1)]**	**20**	**7**	**0.218**	**0.216**
L(18,5)	16	6	0.348	0.123	**SFS[S2:(2,1)(2,1)(3,2)]**	**20**	**6**	**0.173**	**0.232**
L(19,4)	20	8	0.101	0.007	SFS[S2:(2,1)(2,1)(3,4)	24	8	0.122	0.031
L(19,7)	**16**	**7**	**0.384**	**0.361**	SFS[S2:(2,1)(2,1)(3,5)	24	8	0.088	0.050
L(21,8)	**16**	**6**	**0.344**	**0.379**	SFS[S2:(2,1)(2,1)(3,7)	28	10	0.075	0.027
L(22,5)	20	8	0.132	0.010	**SFS[S2:(2,1)(2,1)(4,-1)]**	**20**	**6**	**0.332**	**0.247**
L(23,5)	20	8	0.104	0.006	SFS[S2:(2,1)(2,1)(4,1)]	24	9	0.095	0.012
L(23,7)	**20**	**9**	**0.246**	**0.128**	SFS[S2:(2,1)(2,1)(4,3)]	24	7	0.070	0.057
L(24,7)	**20**	**8**	**0.270**	**0.093**	**SFS[S2:(2,1)(2,1)(5,-3)]**	**20**	**7**	**0.143**	**0.182**
L(25,7)	20	6	0.252	0.055	SFS[S2:(2,1)(2,1)(5,-2)]	20	6	0.242	0.197
L(25,9)	**20**	**9**	**0.268**	**0.204**	SFS[S2:(2,1)(2,1)(5,2)]	24	8	0.055	0.043
L(26,7)	20	7	0.236	0.034	SFS[S2:(2,1)(2,1)(5,3)]	24	7	0.045	0.071
L(27,8)	20	8	0.234	0.075	SFS[S2:(2,1)(2,1)(5,4)]	28	9	0.025	0.005
L(29,8)	20	6	0.216	0.032	SFS[S2:(2,1)(2,1)(7,-5)]	24	9	0.079	0.092
L(29,9)	24	11	0.191	0.091	SFS[S2:(2,1)(2,1)(7,-4)]	24	8	0.138	0.095
L(29,12)	20	7	0.236	0.099	SFS[S2:(2,1)(2,1)(7,-3)]	24	7	0.135	0.012
L(30,7)	24	9	0.121	0.005	SFS[S2:(2,1)(2,1)(7,-2)]	24	8	0.151	0.046
L(30,11)	20	8	0.232	0.179	SFS[S2:(2,1)(2,1)(8,-5)]	24	8	0.112	0.095
L(31,11)	24	11	0.206	0.130	SFS[S2:(2,1)(2,1)(8,-3)]	24	7	0.132	0.035
L(31,12)	20	7	0.214	0.140	SFS[S2:(2,1)(2,1)(9,-7)]	28	11	0.049	0.056
L(33,7)	24	8	0.073	0.002	SFS[S2:(2,1)(2,1)(9,-5)]	28	9	0.065	0.0006
L(33,10)	24	10	0.196	0.063	SFS[S2:(2,1)(2,1)(10,-7)]	28	10	0.067	0.042
L(34,9)	24	9	0.179	0.128	SFS[S2:(2,1)(2,1)(12,-5)]	28	8	0.005	0.00002
L(34,13)	20	6	0.200	0.121	**SFS[S2:(2,1)(3,1)(3,-2)]**	**16**	**5**	**0.334**	**0.500**
L(35,11)	28	13	0.156	0.067	SFS[S2:(2,1)(3,1)(3,-1)]	20	6	0.170	0.138
L(36,11)	24	10	0.182	0.058	SFS[S2:(2,1)(3,1)(3,1)]	24	7	0.147	0.069
L(37,10)	24	8	0.155	0.020	SFS[S2:(2,1)(3,1)(3,2)]	24	7	0.104	0.055
L(39,14)	24	10	0.176	0.102	**SFS[S2:(2,1)(3,1)(4,-3)]**	**20**	**6**	**0.167**	**0.250**
L(41,12)	24	8	0.149	0.014	SFS[S2:(2,1)(3,1)(4,-1)]	24	7	0.193	0.74
L(42,13)	28	12	0.155	0.044	**SFS[S2:(2,1)(3,1)(5,-3)]**	**24**	**7**	**0.164**	**0.228**
L(43,15)	32	15	0.138	0.066	SFS[S2:(2,1)(3,2)(4,-3)]	24	6	0.091	0.022
L(44,13)	24	8	0.122	0.009	SFS[S2:(2,1)(3,2)(4,-1)]	24	7	0.151	0.029
L(48,17)	28	12	0.139	0.061	SFS[S2:(2,1)(3,2)(5,-2)]	24	6	0.067	0.082

References

[1] L. Lindblom, O. Rinne, N. W. Taylor, Building differentiable three-dimensional manifolds numerically, J. Comput. Phys. 410 (2022) 110957.

[2] J. Nocedal, S. J. Wright, Numerical Optimization, Springer, 2006.

[3] B. A. Burton, R. Budney, W. Pettersson, et al., Regina: Software for low-dimensional topology, `http://regina-normal.github.io/`, 1999–2021.